Front. Med. 2022, 16(6): 873−882
https://doi.org/10.1007/s11684-022-0925-2

RESEARCH ARTICLE

Bacteria-mediated tumor-targeted delivery of tumstatin (54-132) significantly suppresses tumor growth in mouse model by inhibiting angiogenesis and promoting apoptosis

Feifei Bao[1], Mengjie Liu[1], Wenhua Gai[1], Yuwei Hua[1], Jing Li[1], Chao Han[1], Ziyu Zai[1], Jiahuang Li[2], Zichun Hua (✉)[1,2]

[1]*The State Key Laboratory of Pharmaceutical Biotechnology, School of Life Sciences, Nanjing University, Nanjing 210023, China;* [2]*Changzhou High-Tech Research Institute of Nanjing University and Jiangsu Target Pharma Laboratories Inc., Changzhou 213164, China*

© Higher Education Press 2022

Abstract **Tumor growth is an angiogenesis-dependent process and accompanied by the formation of hypoxic areas. Tumstatin is a tumor-specific angiogenesis inhibitor that suppresses the proliferation and induces the apoptosis of tumorous vascular endothelial cells. VNP20009, an attenuated *Salmonella typhimurium* strain, preferentially accumulates in the hypoxic areas of solid tumors. In this study, a novel *Salmonella*-mediated targeted expression system of tumstatin (VNP-Tum5) was developed under the control of the hypoxia-induced *J23100* promoter to obtain anti-tumor efficacy in mice. Treatment with VNP-Tum5 effectively suppressed tumor growth and prolonged survival in the mouse model of B16F10 melanoma. VNP-Tum5 exhibited a higher efficacy in inhibiting the proliferation and inducing the necrosis and apoptosis of B16F10 cells *in vitro* and *in vivo* compared with VNP (control). VNP-Tum5 significantly inhibited the proliferation and migration of mouse umbilical vascular endothelial cells to impede angiogenesis. VNP-Tum5 downregulated the expression of anti-vascular endothelial growth factor A, platelet endothelial cell adhesion molecule-1, phosphorylated phosphoinositide 3 kinase, and phosphorylated protein kinase B and upregulated the expression of cleaved-caspase 3 in tumor tissues. This study is the first to use tumstatin-transformed VNP20009 as a tumor-targeted system for treatment of melanoma by combining anti-tumor and anti-angiogenic effects.**

Keywords *Salmonella* VNP20009; tumstatin; B16F10; melanoma; apoptosis; angiogenesis

Introduction

Tumor growth and metastasis depend on adequate blood supply. The growth of tumor cells is autonomous and faster than the formation of new blood vessels, leading to inadequate nutrient and oxygen supply for new blood vessels. Thus, some tumor cells have a low blood flow and form a hypoxia necrosis area [1]. This phenomenon is the theoretical basis for using *Salmonella* as a vector for gene transfer in cancer treatment because it may preferentially localize to and proliferate in hypoxic areas [2,3]. VNP20009, a genetically modified *S. enterica* serovar Typhimurium, was attenuated by deletion of *msbB* and *purI* and underwent phase I clinical trials for metastatic melanomas [4–6]. However, no antitumor activities were reported in the trials [7,8]. To enhance the anti-tumor therapeutic efficacy of *Salmonella*, scholars have developed applications of tumor-targeting VNP 20009 as delivery to overcome the penetration limitation of solid tumor [8] and maximize the activities of genes of interest while reducing systemic toxicity to the host. Mediating the expression of potential genes can further restrict the accumulation of *Salmonella*-delivered anti-tumor agents at the tumor area to achieve the maximum anti-tumor therapeutic efficacy.

Targeting angiogenesis that supports tumor growth rather than tumors themselves may be a promising approach for tumor therapy. Tumstatin is an endogenous angiogenic inhibitor that is generated from type IV collagen [9,10]; it can inhibit the proliferation and

Received May 2, 2021; accepted January 30, 2022
Correspondence: Zichun Hua, zchua@nju.edu.cn

promote the apoptosis of endothelial cells. Maeshima *et al.* [11] reported that the anti-angiogenic activity center of tumstatin is localized to amino acids 54–132 (Tum5), which predominantly binds to the β3 subunit of avβ3 integrin; they also found that tumstatin can inhibit PI3K, FAK, and PKB cell signal transduction pathways [12].

Selective targeting of tumors by hypoxia-selective tumoricidal delivery system increases the concentration of therapeutic genes in tumor while minimizing the damage to normal tissues. A controllable delivery system is used to manage the timing and location of protein expression *in vivo*. The anaerobic-inducible and constitutive *J23100* promoter can be heterologously expressed in facultative anaerobes and shows excellent stability [13]. In this perspective, we selected VNP20009 as a carrier to deliver Tum5 under the control of the *J23100* promoter (VNP-Tum5) for treatment of melanoma in a mouse model. The selective accumulation of engineered VNP20009 to express tumstatin may avoid unintended toxicities for normal tissues, such as liver and spleen, thereby enhancing the anti-tumor efficacy. The present study explored the anti-tumor effect and possible mechanisms of VNP-Tum5 on a mouse model of B16F10 melanoma *in vitro* and *in vivo*. *Salmonella*-mediated tumor-targeted tumstatin gene therapy significantly suppressed tumor growth and extended host survival. Results provide a preclinical proof-of-principle that VNP-Tum5 has better anti-tumor and anti-angiogenic effects than VNP *in vitro* and *in vivo*. Hence, Tum-load *Salmonella* is a potential therapeutic approach in oncotherapy. This work is the first to report the use of Tum5-transformed VNP20009 as a specific gene delivery system for tumor treatment.

Materials and methods

Bacterial strains, tumor cell lines, and animals

The bacterial strain VNP20009 and B16F10 melanoma were obtained from ATCC (USA). MUVECs were purchased from Hefei Bomei Biotechnology Co., Ltd. (Hefei, China). All the strains used in this study were grown in Luria-Bertani broth at 37 °C. B16F10 melanoma cells and MUVECs were cultured in 5% CO_2 at 37 °C in high-glucose DMEM (Sigma-Aldrich, Shanghai, China) supplemented with 10% fetal bovine serum (Hyclone, USA), streptomycin (100 μg/mL), and penicillin (100 IU/mL). Female C57BL/6 mice, 6–8 weeks old, were obtained from the Comparative Medicine Center of Yangzhou University (Yangzhou, China) and maintained under a sterile environment condition for 1 week before the start of the experiment. This study was approved by the Animal Care and Use Committee of Nanjing University and carried out following the Guide for the Care and Use of Laboratory Animals by the National Research Council.

Plasmid construction and bacterial transformation

Tum5 (tumstatin, 54–132 aa) was amplified by primers Tum-sense and Tum-antisense. The primer sequences were as follows: Tum-sense, 5′-cggcagcggaggtggaggcagc-ggaaatgaacaagcccatgga-3′; Tum-antisense, 5′-ctggtacta-gtggatccttaaatcgtaggaccttcacagaca-3′. The Tum5 sequence was cloned into the prokaryotic expression vector pTh01 (maintained in our laboratory) by using a one-step cloning kit (Vazyme Biotech, Nanjing, China) under the control of the *J23100* promoter to obtain plasmid pTh21-Tum5. The positive clones were confirmed by DNA sequencing (Sangon Biotech, Shanghai, China). The pTh01 and pTh21-Tum5 plasmids were transformed into VNP20009 by using Gene Pulser Xcell™ (Bio-Rad, CA, USA) at 25 μF, 1.8 kV, and 400 Ω and plated on LB agar containing 50 μg/mL kanamycin. Positive VNP20009 was named VNP and VNP-Tum5.

Construction of mouse tumor model

Female wild-type C57BL/6 (6–8 weeks old) mice were inoculated subcutaneously with 5×10^5 B16F10 melanoma cells in 0.1 mL of PBS on the mid-right flank. Mice with B16F10 melanoma and tumor volume of about 100 mm^3 (at day 7 post tumor inoculation) were randomly divided into three groups: VNP-Tum5, VNP, and PBS. Mice in the VNP-Tum5 and VNP groups were treated intraperitoneally with *S. typhimurium* strains VNP-Tum5 or VNP at a dose of 1×10^6 CFU in 0.1 mL of PBS, respectively [14,15]. Mice in the PBS group were injected with 0.1 mL of PBS and used as control (n = 12 in each group). The width and length of the tumor were recorded every 3 days. The number and dates of death of mice were recorded to calculate survival rate. Tumor volume was determined using the formula: tumor volume = length × $width^2$ × 0.52. Assuming that changes in the tumor volume are exponential, a regression line, $\lg y = \lg a + bx$ (x, days after the baseline radiologic image; y, tumor volume), was calculated by nonlinear square regression. The doubling time (DT) of tumor volume was defined as (lg2)/b. DT was calculated from the baseline image and historical image obtained before. Tumor growth delay (TGD) was calculated as the time taken by each individual tumor to reach 800 mm^3 in the treatment groups compared with that in the untreated controls. The mice were sacrificed at day 13 post tumor inoculation (n = 4 in each group). Tumor tissues, spleen, and liver were collected.

Staining and microscopy

An B16F10 melanoma mouse model was used to

understand the treatment properties of VNP-Tum5. After bacterial treatment for 6 days, mice in the VNP-Tum5, VNP, and PBS groups were sacrificed to determine the mechanism of the recombined bacteria. The tumor, spleen, and liver tissues were fixed in 10% paraformaldehyde (PFA) overnight, paraffin-embedded, sectioned, fixed on slides (thickness of 5 μm), and prepared according to the standard manufacturing procedures for paraffin sections. Hematoxylin–Eosin (HE) staining was carried out by HE Staining Kit (Solarbio Life Science, Beijing, China). TdT-mediated dUTP Nick-End Labeling (TUNEL) assays were carried out by detecting the apoptotic nuclei on TUNEL BrightGreen Apoptosis Detection Kit (Vazyme Biotech, Nanjing, China) following the manufacturer's instructions. Ki67 mouse mAb (#9449) and CD31 Rabbit mAb (#77699) were acquired from CST Technology. After staining, the relative fluorescence intensity was quantified by ImageJ software (NIH, Bethesda, MD, USA).

In vitro cell migration assay

MUVECs were seeded into six-well plates at 2×10^5 cells/well and cultured with 10% FBS overnight. After washing twice with PBS, the monolayers were wounded in a line across the well with a 10 μL standard pipette tip and then incubated with VNP and VNP-Tum5 in the absence of serum media. Photographs of migration into open wounds were taken at different time points until the scratches were almost closed.

Western blot analysis

The tissues were lysed in RIPA buffer (Santa Cruz Biotechnology) supplemented with 1 μL of protease inhibitor cocktail (Cell Signaling, USA) and incubated on ice for about 30 min. Protein concentration was calculated using the BCA Protein Quantification Kit (Vazyme Biotech, Nanjing, China). About 50 μg of total protein was used for Western blot analysis following standard conditions with primary antibodies as follows: diluted 1:1000 for VEGF-A (#19003-1-AP, Proteintech Group, Wuhan, China), 1:1000 for GAPDH (#2819, Santa, Shanghai, China), Flag (#18230, Abcam, Cambridge, USA), VEGFR-2 (#9698, CST, Shanghai, China), AKT (#4085S, CST, Shanghai, China), p-AKT (#9275S, CST, Shanghai, China), PI3K (#4292S, CST, Shanghai, China), p-PI3K (#17366S, CST, Shanghai, China), caspase 3 (#9662S, CST, Shanghai, China), and p-caspase 3 (#17366S, CST, Shanghai, China). Detection was performed with ECL plus Western blot detection system (Tanon, Shanghai, China). The tumor tissues were homogenized in lysis buffer and incubated on ice for about 30 min. The sample was centrifuged, and the supernatant was used for Western blot analysis. Intensity was quantitatively analyzed by ImageJ software.

Flow cytometry analysis of cell apoptosis

2×10^5 B16F10 cells were seeded in a 12-well plate for about 12 h to reach a density of 70%–80% and treated with different bacteria for 2 h and 4 h. Cells were harvested by trypsinization, washed with cold PBS, and stained with EGFP-annexin V in binding buffer for 15–20 min and propidium iodide for 5 min. The results were analyzed using Flow Cytometer (BD FACSCanto II). Apoptosis rate was analyzed with FlowJo analysis software (Tree Star, Ashland, OR, USA). Three independent experiments were conducted, and each experiment was repeated twice.

Cell toxicity assay

MTT (Thiazolyl Blue Tetrazolium Bromide) assay was used to determine anti-proliferative effects on endothelial cells [16]. In brief, 5×10^3 MUVECs were seeded in a 96-well plate for 12 h to reach a density of 70%–80% and then treated with *Salmonella* for 2 h at different MOI (1:10, 1:50, 1:100). Absorbance was recorded at 490 nm.

Statistical analysis

All data were expressed as mean ± SD after analysis with GraphPad Prism 8.0 (Graph Pad Software, San Diego, CA, USA). The effect of treatment on survival time was determined using log-rank test. Paired Student's *t*-test analysis was used to estimate statistical differences among groups. $P < 0.05$ was considered to indicate statistical significance.

Results

VNP-Tum5 inhibited tumor growth and prolonged survival time

In bacteria-based anticancer therapy, maintaining functional gene expression in the hypoxic tumor regions is essential. In our previous work, we constructed the pTh01 plasmid with a strong promoter *J23100*, a bacterial signal peptide that ensures protein expression, and a Flag tag, which is a kanamycin resistance selection marker (Fig. 1A). As shown in Fig. 1B, the Tum5-Flag protein was successfully expressed in melanoma tissues.

The anti-tumor effects of *Salmonella* strain VNP and VNP-Tum5 were determined on B16F10 mouse model. In mice treated with VNP-Tum5 (1×10^6 CFU), tumor growth was suppressed (Fig. 1C) and survival was prolonged (Fig. 1E). At sacrifice time, B16F10 melanoma (day 13) in the VNP-Tum5 group reached an average tumor volume of 737 mm^3, while that in the VNP group was 1235 mm^3 (1.67-fold). The tumor sizes were lower in

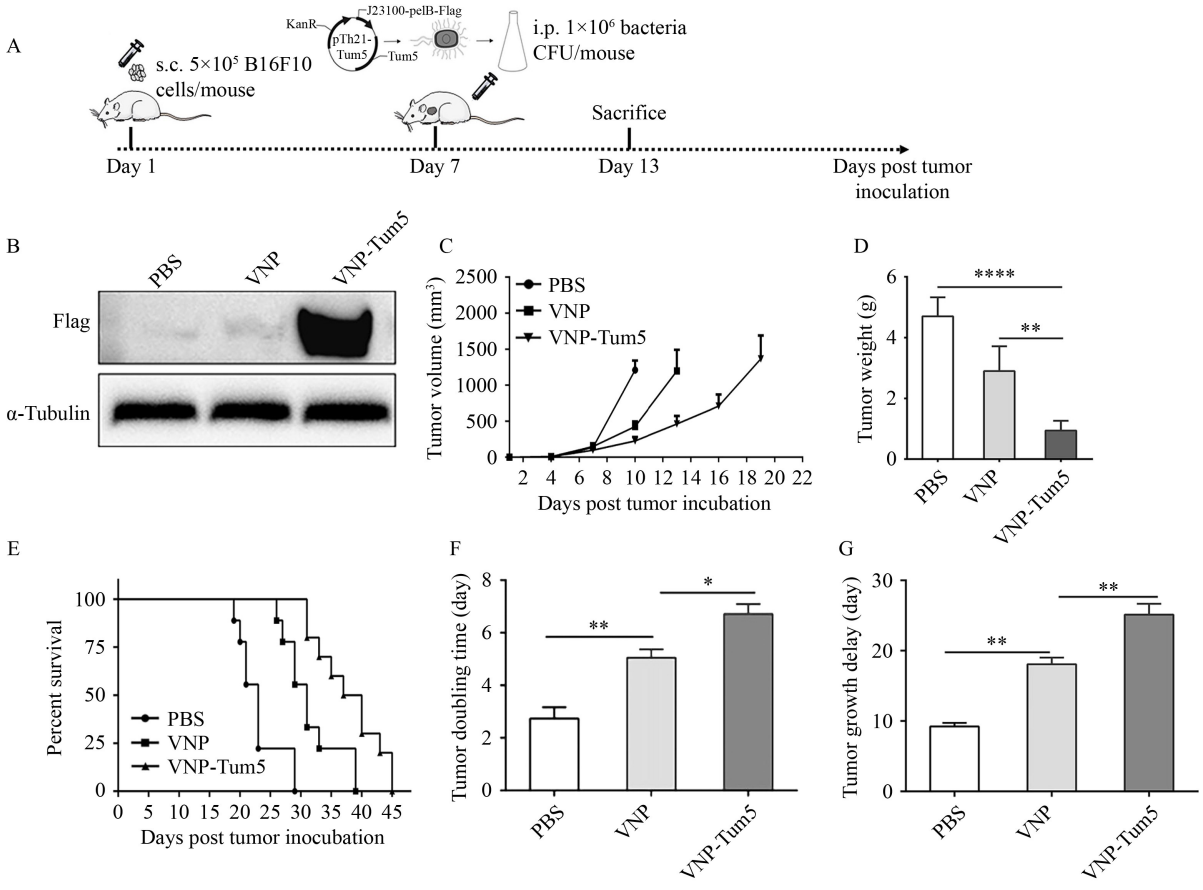

Fig. 1 VNP-Tum5 and VNP delayed tumor growth and enhanced survival time in the melanoma tumor model of mice. (A) Schematic representation of the production of VNP-Tum5 and the treatment schedule. B16F10 tumor mice (n = 12 in each group) were injected i.p. with 1×10^6 CFU of VNP, VNP-Tum5, or with 100 μL of PBS on day 7. (B) Detection of the expression of Tum5 in the tumor tissues of mice bearing melanoma by Western blot. α-Tubulin served as the loading control (n = 4). (C) Tumor growth curves (n = 10). (D) Representative efficacy of the recombinant VNP20009 in melanoma therapy (n = 4). (E) Kaplan–Meier survival curves of tumor-bearing mice after different treatments (n = 12). (F) Tumor doubling time of the mice. (G) Tumor growth delay of the mice (n = 8). Tumor data among different groups were compared. Data are presented as mean ± SD. $^*P < 0.05$, $^{**}P < 0.01$, $^{****}P < 0.0001$.

the treatment groups than in the control group (treated with PBS). The average tumor weight in the VNP-Tum5 group (1.35 g) was reduced compared with that in the VNP group (2.45 g, Fig. 1D). Moreover, VNP-Tum5 significantly prolonged the overall survival (Fig. 1E). The tumor DT (7.3 days, Fig. 1F) and TGD (23.2 days, Fig. 1G) were significantly increased in mice treated with VNP-Tum5 than in the VNP group (4.6 days and 18.4 days, respectively). Overall, VNP-Tum5 led to stronger tumor growth inhibition than VNP.

Colonization and toxicological risk assessment of VNP-Tum5 in tumor-bearing mice

As shown in Fig. 2A, the colony formation assays of VNP-Tum5 in the tumor, spleen, and liver tissues demonstrated that the exact number of tumor-colonized bacteria was not improved in the VNP group. The relative tumor specificity of VNP-Tum5 to the liver was improved to 2500:1; a previous study reported that VNP20009 had a tumor-to-liver ratio of bacterial colonization of about 1000:1 [17]. The results demonstrated that the expression system under the control of the hypoxia-induced *J23100* promoter could enhance the targeted efficacy.

As shown in Fig. 2B and 2C, the Tum5-Flag protein was successfully expressed in the spleen and liver. Treatment with VNP-Tum5 did not change the weight of the body (Fig. 2J), spleen (Fig. 2D and 2E), and liver (Fig. 2F and 2G) compared with VNP. However, the weights of the spleen (Fig. 2E) and liver (Fig. 2F) in the VNP-Tum5 and VNP groups were higher than those in the PBS group. The body weight of tumor-bearing mice was then examined on day 5 after bacterial therapy. A steady decrease of approximately 15% in body weight was found in mice treated with *Salmonella* (Fig. 2J) compared with PBS. Additionally, the HE staining of the liver and spleen (Fig. 2H and 2I) displayed no necrosis areas in the VNP-Tum5 and VNP groups. Hence,

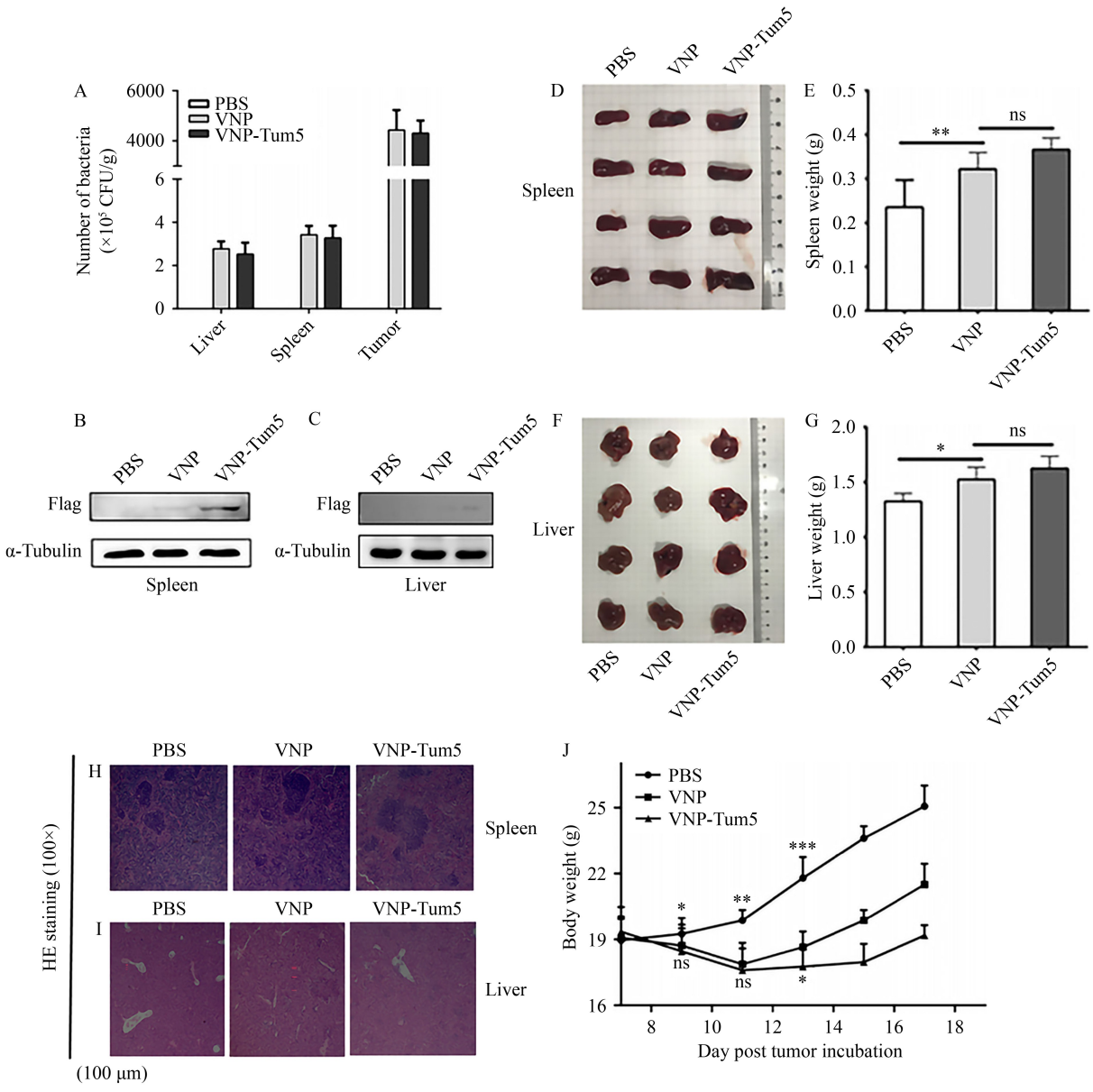

Fig. 2 Toxicological assessment of VNP-Tum5 and VNP in melanoma tumor mouse model. (A) Number of bacteria that colonized the tumors, spleen, and liver at day 6 post-infection (n = 4). (B) Detection of Tum5 expression in the spleen of mice bearing melanoma by Western blot analysis. α-Tubulin served as loading control (n = 3). (C) Detection of Tum5 expression in the liver of mice bearing melanoma by Western blot analysis. α-Tubulin served as loading control (n = 3). (D, E) Spleen and spleen weight after tumor incubation for 13 days (n = 4). (F, G) Liver and liver weight after tumor incubation for 13 days (n = 4). (H, I) HE staining of the spleen and liver tissues (n = 3). (J) Variations in body weight after bacterial infection. The P value was significant between the VNP group and the PBS group. Data are presented as mean ± SD. *P < 0.05, **P < 0.01, ***P < 0.001. ns, no significance.

VNP-Tum5 has no potential toxic side effects compared with VNP.

VNP-Tum5 induced the apoptosis and necrosis of melanoma *in vivo* and *in vitro*

The histochemistry scores (Fig. 3A and 3B) showed that all groups had tumor necrosis region, while VNP-Tum5 formed more necrosis areas (63.5%) than VNP (39.8%). The TUNEL analysis revealed that the tumor tissues in the VNP-Tum5 group had higher apoptosis rate (36.5%) than that in the VNP group (24.2%, Fig. 3C and 3E). VNP-Tum5 could induce more melanoma cells to undergo apoptosis. Tumor proliferation was also assessed by immunofluorescence using an antibody against murine Ki67 (Fig. 3C). VNP-Tum5 can inhibit tumor proliferation rate by 17.2% compared with VNP (P < 0.01, Fig. 3C and 3D).

After B16F10 cells were treated with PBS, VNP, and VNP-Tum5 for 2 h and 4 h, the rates of apoptosis and

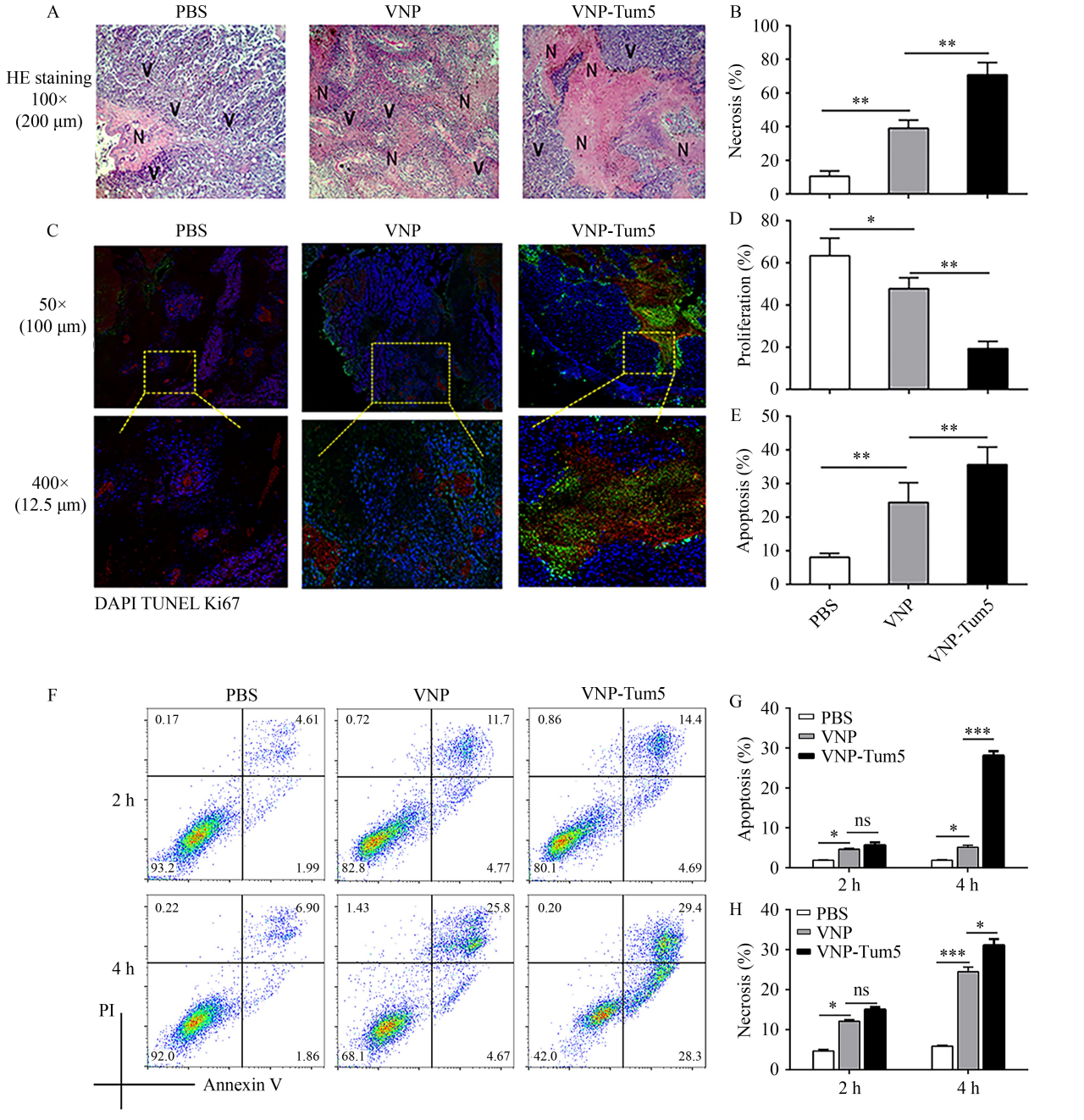

Fig. 3 VNP-Tum5 and VNP induced the apoptosis and necrosis of melanoma *in vivo* and *in vitro*. (A) HE staining of tumor tissues (n = 3). Representative images (100×) reveal tumor necrotic areas of B16F10 tumor section treated with PBS, VNP, and VNP-Tum5 (vital tumor regions, V; necrotic tumor regions, N). (B) Quantification of necrotic tumor tissue (n = 3). (C) Ki67 and TUNEL assay of tumor tissue. Representative images showing cell proliferation and apoptosis in tumor tissues with different treatments (bright blue, nuclei; bright green, apoptotic cells; bright red, tumor aggressiveness). (D and E) Quantification of proliferation and apoptosis levels of tumor tissues (n = 3). Quantification of fluorescence by ImageJ software. (F) Representative FACS analysis of annexin V and propidium iodide (PI) staining after 2 h and 4 h of incubation with the strains (n = 3). (G, H) Quantification of apoptosis and necrosis of B16F10 melanoma cells after 2 h and 4 h of incubation with the strains (n = 3). Bar represents mean ± SD of five optical fields. *P < 0.05, **P < 0.01. ***P < 0.001. ns, no significance.

necrosis were analyzed by flow cytometry (Fig. 3F). The apoptosis and necrosis rates were significantly increased by 19.2% (P < 0.001, Fig. 3G) and 3.5% (P < 0.05, Fig. 3H), respectively, in the VNP-Tum5 group at 4 h compared with those in the VNP group. Statistical analysis showed no significant difference in the apoptosis and necrosis rates after treatment at 2 h (Fig. 3G and 3H). Hence, VNP-Tum5 could induce more apoptosis and necrosis of melanoma *in vivo* and *in vitro*. Moreover, the synergistic tumor inhibition effects of VNP-Tum5 could be partially attributed to the enhanced apoptosis and necrosis of melanoma cells.

VNP-Tum5 targeted tumor vessels and inhibited angiogenesis by downregulating VEGF-A

Tumor necrosis is usually caused by insufficient blood supply; in this regard, whether VNP-Tum5 affects tumor angiogenesis should be investigated. The blood vessel density of melanoma tumor tissue was evaluated by immunofluorescence using an antibody against mouse CD31, a well-recognized marker of angiogenesis (Fig. 4A). The vascular density of tumors treated with VNP-Tum5 was significantly decreased by about 6% compared with that of tumors treated with VNP (Fig. 4B). To determine the mechanism underlying the lower microvascular densities induced by VNP-Tum5, we detected the vascular endothelial growth factor (VEGF-A) levels of the tumor (Fig. 4C and 4D). As expected, the expression of VEGF-A was decreased by about 1.9-fold by VNP-Tum5 treatment ($P < 0.05$, Fig. 4D).

VNP-Tum5 inhibited the migration and proliferation of MUVECs

A series of experiments was conducted on MUVECs to investigate the antiangiogenic activity of VNP-Tum5 *in vitro* (MOI = 10:1). First, we examined the effect of VNP-Tum5 on MUVEC motility by wound healing scratching assay (Fig. 4E). Quantitative analysis revealed that VNP-Tum5 effectively hindered the healing process by 47.8%, which was higher than that in the VNP group (22.6%, $P < 0.001$, Fig. 4F).

The effect of VNP-Tum5 and VNP on the proliferation of MUVECs was assessed using MTT assay. As shown in Fig. 4G, the inhibition rates of VNP-Tum5 at MOIs of 100:1, 50:1 and 10:1 were increased by 9.1% ($P < 0.001$), 7.3% ($P < 0.01$), and 0.7% ($P > 0.01$), respectively, compared with VNP. In summary, the inhibition of MUVEC proliferation was stronger in the VNP-Tum5 group than in the VNP group. Moreover, the inhibition rate increased in a dose-dependent manner with increasing MOI. Collectively, these results suggest that VNP-Tum5 could significantly inhibit the migration and proliferation of MUVECs *in vitro*.

VNP-Tum5 induced apoptosis by inhibiting the VEGFR2/PI3K/AKT pathway

The vascular endothelial growth factor (VEGF-A) levels in tumor tissues treated with VNP were measured to

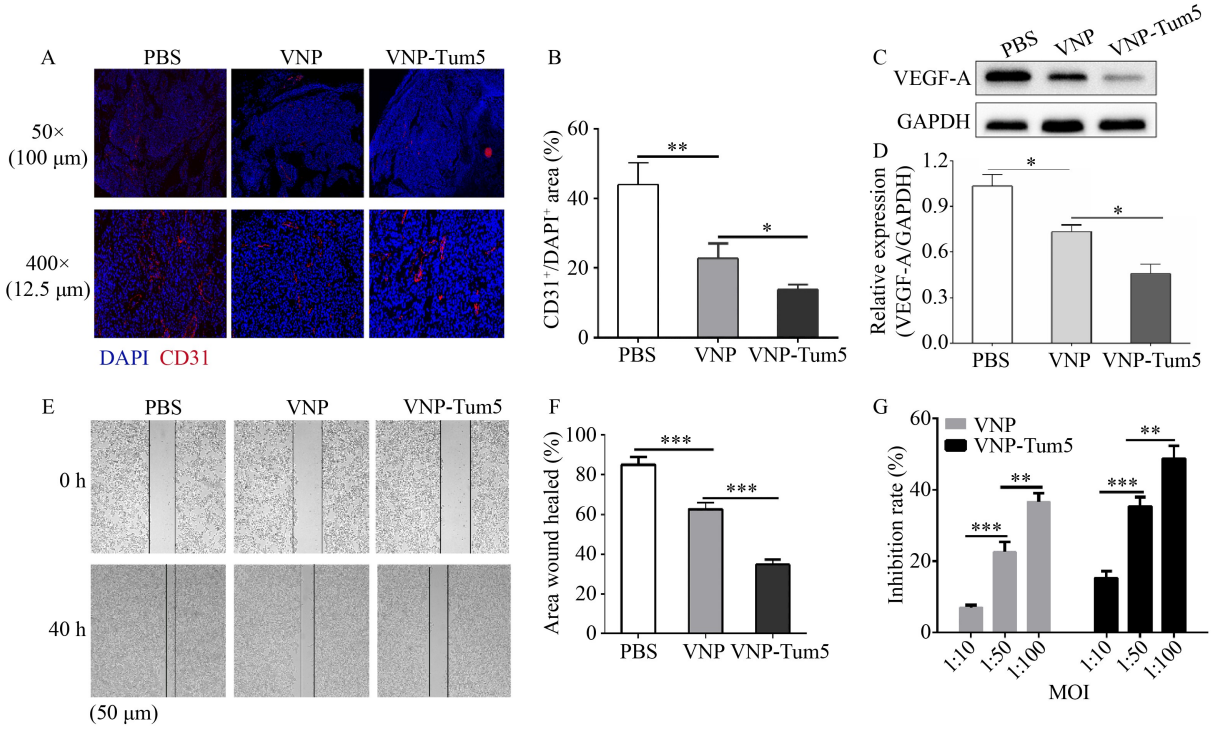

Fig. 4 VNP-Tum5 and VNP targeted at tumor blood vessels, inhibited proliferation, and inhibited angiogenesis on MUVECs. (A) Fluorescence images of tumor blood vessels. Blood vessel staining was performed and showed the co-localization of CD31 (red) and DAPI (blue) in tumor samples. (B) Quantification of CD31-positive tumor vessels. (C) VEGF-A expression in xenograft tumors from different groups at the protein level monitored by Western blot analysis. (D) Statistical analysis of VEGF-A results determined by Western blot by ImageJ. (E) Wound healing assay of MUVECs after incubation with the strain for 2 h (MOI = 1:10). (F) Statistical analysis of the wound healing experiment of MUVECs by ImageJ. (G) Inhibition of VNP and VNP-Tum5 on MUVECs at different MOI. Data are shown as mean ± SD ($n = 3$) with individual data points shown, analyzed by two-tailed *t*-test. *$P < 0.05$; **$P < 0.01$; ***$P < 0.001$.

determine the mechanism of lower microvascular densities caused by VNP-Tum5. As expected, VEGF-A in the tumor tissues was inhibited by VNP-Tum5 therapy (Fig. 4C), suggesting the potential regulatory role of VEGF-A by VNP-Tum5. To determine the signaling pathways associated with VEGF-A in mediating apoptosis, we examined the expression of VEGFR2 and its downstream pathway molecules such as PI3K and AKT (Fig. 5A). Treatment with VNP-Tum5 obviously decreased the phosphorylation of PI3K and AKT proteins (Fig. 5A). The levels of PI3K and AKT were not changed or even reduced, and the total protein expression levels were kept unchanged (Fig. 5A), suggesting that VEGFR2 was responsible for the inhibition of the phosphorylation of PI3K and AKT molecules. In addition, the protein expression levels of p-PI3K/PI3K and p-AKT/AKT were significantly reduced in the VNP-Tum5 group.

Discussion

Tumor development may be determined by the relative levels of pro-angiogenic factors and anti-angiogenic factors, which are in a balanced state under normal physiologic conditions [18]. The transformation from *in situ* tumor to malignancy may involve a transformation of neovascularization, so gene-regulated endogenous angiogenesis inhibitors at the physiologic level may serve as a checkpoint for tumor growth [19]. Tumstatin is a potential antitumor drug due to its dual mechanism of anti-tumor angiogenesis and inhibition of tumor cell proliferation [20,21]. Compared with common anti-tumor drugs, tumstatin has the following advantages. (1) Tumstatin has fewer side effects because it is a small fragment of endogenous protein (28 kDa) and is a highly conserved molecule that does not normally produce toxicity [22,23]. (2) Tumstatin has less drug resistance because it targets vascular endothelial cells where genes are more stable than tumor cells [11]. (3) Tumstatin has high specificity because it specifically inhibits tumor angiogenesis without affecting physiologic angiogenesis [24]. (4) Tumstatin has high anti-tumor effect because it can target blood vessels to induce tumor tissue necrosis and prevent tumor metastasis to achieve better anti-tumor effect [25,26]. Thus, tumstatin is a promising therapeutic candidate in the control of tumor angiogenesis and growth.

Anaerobic *Salmonella* can selectively colonize tumors, inhibit tumor growth, and prolong survival after systemic infection in animal tumor models [6,27,28]. The effectiveness of engineered attenuated *S. typhimurium* strain, which was employed as live delivery vectors of various antitumor therapeutic agents or combined with other therapies, has been evaluated in a large number of animal experiments [2,29,30]. For example, the well-known genetically engineered *S. typhimurium* strain VNP20009 ($purI^{-}/msbB^{-}$) was attenuated by more than 10 000-fold compared with the wild-type strain [14,17,31,32]. VNP20009 has an excellent safety profile in rodents and dogs and was thus subjected to phase I clinical trials, which documented the safety of the bacterial regimen in patients with cancers [7,33]. However, VNP20009 showed insufficient tumor colonization and weak biological effects, and none of the patients experienced obvious tumor regression [7].

In this study, we investigated whether tumstatin could exert high antiangiogenesis effects when used with VNP20009 as a delivery system to achieve better inhibitory effect on tumor growth in melanoma-bearing mice. We developed a bacteria-mediated system under the control of the hypoxia-induced *J23100* promoter to

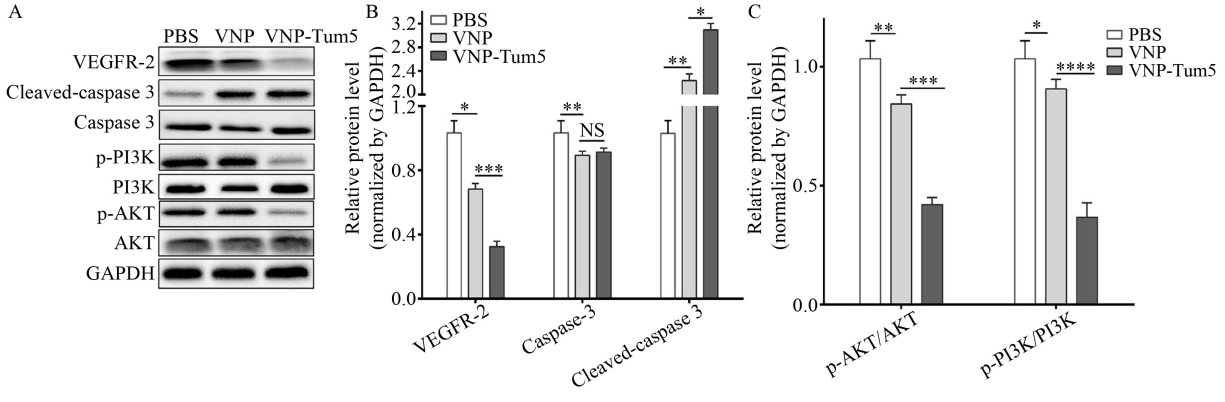

Fig. 5 Mechanism of VNP-Tum5 and VNP on melanoma is associated with VEGF-A/VEGFR-2 and PI3K-AKT signaling pathways in tumor tissues. (A) Relative expression levels of VEGFR2, caspase 3, clevavead-caspase 3, p-PI3K/PI3K, and p-AKT/AKT were determined by Western blot analysis (n = 3). (B, C) Statistical analysis of the results of Western blot by ImageJ. (D) Possible mechanism of VNP-Tum5 in inhibiting melanoma. Data are presented as mean ± SD with individual data points shown, analyzed by two-tailed t-test. *P < 0.05; **P < 0.01; ***P < 0.001, ****P < 0.0001.

express the amino acids 54–132, where the antiangiogenic activity of the tumstatin protein is located [11].

Treatments using 10^6 CFU engineered *Salmonella* induced toxicity (Fig. 2). The combination of tumstatin and VNP20009 could be a safe option and has no serious side effects. Therefore, using VNP20009 as a vector to deliver tumstatin may provide a promising therapeutic regimen for melanoma.

The results of the examination of tumor volume and histological changes at macroscopic and microscopic levels showed that Tum5 inhibited tumor growth due to the transgenic expression of Tum5. The vector group VNP failed to exhibit similar effects. The TUNEL and Ki67 assays showed that VNP-Tum5 was associated with significant apoptotic activities and suppressed the proliferation of melanoma cells *in vivo* and *in vitro*, which could contribute to the tumor inhibitory effects and survival benefit observed in this study.

The VNP20009 delivery of Tum5 markedly restrained the tumor angiogenesis. We demonstrate the possibility of significantly reducing CD31 levels in tumor tissues. To confirm the mechanisms of apoptosis induction, proliferation inhibition, and anti-angiogenesis activity by VNP-Tum5, we designed a series of experiments *in vitro*. VNP-Tum5 induced the apoptosis of B16F10 cells. The wound healing and MTT assays on MUVECs showed that VNP-Tum5 inhibited cell migration and proliferation. Thus, VNP-Tum5 exerted an antitumor effect via several mechanisms: inducing tumor apoptosis and suppressing tumor migration. In addition, we evaluated the expression of apoptotic effector caspase 3 and the changes in VEGFR2, p-PI3K, P13K, p-AKT, and AKT on tumor tissues. The expression of cleaved caspase 3 increased, and those of VEGFR2, p-AKT/AKT, p-PI3K/P13K decreased. These results suggest that the antitumor effects of the engineered bacteria may be at least partially mediated by the VEGF-A/VEGFR-2 and P13K-AKT signaling pathways.

To our knowledge, this study is the first to report the tumor suppression and anti-angiogenic effects of VNP20009 used as a delivery vector for the protein tumstatin *in vivo* and *in vitro*. VNP-Tum5 therapy could serve as a prototype for further development of a feasible and effective option for treatment of melanoma.

Acknowledgements

This study was supported in part by grants from the National Natural Sciences Foundation of China (No. 82130106) and the Jiangsu Provincial Department of Science and Technology (No. BK20192005).

Compliance with ethics guidelines

Feifei Bao, Mengjie Liu, Wenhua Gai, Yuwei Hua, Jing Li, Chao Han, Ziyu Zai, Jiahuang Li, and Zichun Hua declared no potential conflicts of interest to disclose. The study involved animals that were maintained and treated in accordance with Chinese legal requirements. The experiments were approved by Nanjing University Animal Care and Use Committee, and the rules were strictly followed during the experiments.

References

1. Hanahan D, Folkman J. Patterns and emerging mechanisms of the angiogenic switch during tumorigenesis. Cell 1996; 86(3): 353–364
2. Jazowiecka-Rakus J, Szala S. Antitumour activity of *Salmonella typhimurium* VNP20047 in B16(F10) murine melanoma model. Acta Biochim Pol 2004; 51(3): 851–856
3. Low KB, Ittensohn M, Luo X, Zheng LM, King I, Pawelek JM, Bermudes D. Construction of VNP20009: a novel, genetically stable antibiotic-sensitive strain of tumor-targeting Salmonella for parenteral administration in humans. Methods Mol Med 2004; 90: 47–60
4. Zheng JH, Min JJ. Targeted cancer therapy using engineered *Salmonella typhimurium*. Chonnam Med J 2016; 52(3): 173–184
5. Kimura H, Zhang L, Zhao M, Hayashi K, Tsuchiya H, Tomita K, Bouvet M, Wessels J, Hoffman RM. Targeted therapy of spinal cord glioma with a genetically modified *Salmonella typhimurium*. Cell Prolif 2010; 43(1): 41–48
6. Luo X, Li Z, Lin S, Le T, Ittensohn M, Bermudes D, Runyab JD, Shen SY, Chen J, King IC, Zheng LM. Antitumor effect of VNP20009, an attenuated *Salmonella*, in murine tumor models. Oncol Res 2001; 12(11−12): 501−508
7. Toso JF, Gill VJ, Hwu P, Marincola FM, Restifo NP, Schwartzentruber DJ, Sherry RM, Topalian SL, Yang JC, Stock F, Freezer LJ, Morton KE, Seipp C, Haworth L, Mavroukakis S, White D, MacDonald S, Mao J, Sznol M, Rosenberg SA. Phase I study of the intravenous administration of attenuated *Salmonella typhimurium* to patients with metastatic melanoma. J Clin Oncol 2002; 20(1): 142–152
8. Forbes NS, Munn LL, Fukumura D, Jain RK. Sparse initial entrapment of systemically injected *Salmonella typhimurium* leads to heterogeneous accumulation within tumors. Cancer Res 2003; 63(17): 5188–5193
9. Floquet N, Pasco S, Ramont L, Derreumaux P, Laronze JY, Nuzillard JM, Maquart FX, Alix AJ, Monboisse JC. The antitumor properties of the α3(IV)-(185-203) peptide from the NC1 domain of type IV collagen (tumstatin) are conformation-dependent. J Biol Chem 2004; 279(3): 2091–2100
10. Van der Velden J, Harkness LM, Barker DM, Barcham GJ, Ugalde CL, Koumoundouros E, Bao H, Organ LA, Tokanovic A, Burgess JK, Snibson KJ. The effects of tumstatin on vascularity, airway inflammation and lung function in an experimental sheep model of chronic asthma. Sci Rep 2016; 6(1): 26309
11. Maeshima Y, Manfredi M, Reimer C, Holthaus KA, Hopfer H, Chandamuri BR, Kharbanda S, Kalluri R. Identification of the anti-angiogenic site within vascular basement membrane-derived tumstatin. J Biol Chem 2001; 276(18): 15240–15248
12. Kawaguchi T, Yamashita Y, Kanamori M, Endersby R,

Bankiewicz KS, Baker SJ, Bergers G, Pieper RO. The PTEN/Akt pathway dictates the direct αVβ3-dependent growth-inhibitory action of an active fragment of tumstatin in glioma cells *in vitro* and *in vivo*. Cancer Res 2006; 66(23): 11331–11340

13. Wahyu Effendi SS, Tan SI, Ting WW, Ng IS. Enhanced recombinant *Sulfurihydrogenibium yellowstonense* carbonic anhydrase activity and thermostability by chaperone GroELS for carbon dioxide biomineralization. Chemosphere 2021; 271: 128461
14. Chen T, Zhao X, Ren Y, Wang Y, Tang X, Tian P, Wang H, Xin H. Triptolide modulates tumour-colonisation and anti-tumour effect of attenuated *Salmonella* encoding DNase I. Appl Microbiol Biotechnol 2019; 103(2): 929–939
15. Zhang X, Cheng X, Lai Y, Zhou Y, Cao W, Hua ZC. Salmonella VNP20009-mediated RNA interference of ABCB5 moderated chemoresistance of melanoma stem cell and suppressed tumor growth more potently. Oncotarget 2016; 7(12): 14940–14950
16. Jiang XD, Qiao Y, Dai P, Chen Q, Wu J, Song DA, Li SQ. Enhancement of recombinant human endostatin on the radiosensitivity of human pulmonary adenocarcinoma A549 cells and its mechanism. J Biomed Biotechnol 2012; 2012: 301931
17. Clairmont C, Lee KC, Pike J, Ittensohn M, Low KB, Pawelek J, Bermudes D, Brecher SM, Margitich D, Turnier J, Li Z, Luo X, King I, Zheng LM. Biodistribution and genetic stability of the novel antitumor agent VNP20009, a genetically modified strain of *Salmonella typhimurium*. J Infect Dis 2000; 181(6): 1996–2002
18. Sottile J. Regulation of angiogenesis by extracellular matrix. Biochim Biophys Acta 2004; 1654(1): 13–22
19. Hlatky L, Hahnfeldt P, Folkman J. Clinical application of antiangiogenic therapy: microvessel density, what it does and doesn't tell us. J Natl Cancer Inst 2002; 94(12): 883–893
20. Li W, Zhai L, Tang Y, Cai J, Liu M, Zhang J. Antitumor properties of taxol in combination with cyclooxygenase-1 and cyclooxygenase-2 selective inhibitors on ovarian tumor growth *in vivo*. Oncol Res 2012; 20(2−3): 49−59
21. Maeshima Y, Sudhakar A, Lively JC, Ueki K, Kharbanda S, Kahn CR, Sonenberg N, Hynes RO, Kalluri R. Tumstatin, an endothelial cell-specific inhibitor of protein synthesis. Science 2002; 295(5552): 140–143
22. Hamano Y, Kalluri R. Tumstatin, the NC1 domain of α3 chain of type IV collagen, is an endogenous inhibitor of pathological angiogenesis and suppresses tumor growth. Biochem Biophys Res Commun 2005; 333(2): 292–298
23. Gu Q, Zhang T, Luo J, Wang F. Expression, purification, and bioactivity of human tumstatin from *Escherichia coli*. Protein Expr Purif 2006; 47(2): 461–466
24. Hamano Y, Zeisberg M, Sugimoto H, Lively JC, Maeshima Y, Yang C, Hynes RO, Werb Z, Sudhakar A, Kalluri R. Physiological levels of tumstatin, a fragment of collagen IV α3 chain, are generated by MMP-9 proteolysis and suppress angiogenesis via αV β3 integrin. Cancer Cell 2003; 3(6): 589–601
25. Zhang GM, Sui LH, Jia T, Zhao YZ, Fu SB, Liu XH, Yu Y. Inhibitory effect of recombinant anti-angiogenic peptide of tumstatin on growth and metastasis of human ovarian cancer transplanted in nude mice. Chin J Oncol (Zhonghua Zhong Liu Za Zhi) 2008; 30(3): 170−173 (in Chinese)
26. Sudhakar A, Boosani CS. Inhibition of tumor angiogenesis by tumstatin: insights into signaling mechanisms and implications in cancer regression. Pharm Res 2008; 25(12): 2731–2739
27. Weth R, Christ O, Stevanovic S, Zöller M. Gene delivery by attenuated *Salmonella typhimurium*: comparing the efficacy of helper versus cytotoxic T cell priming in tumor vaccination. Cancer Gene Ther 2001; 8(8): 599–611
28. Tjuvajev J, Blasberg R, Luo X, Zheng LM, King I, Bermudes D. *Salmonella*-based tumor-targeted cancer therapy: tumor amplified protein expression therapy (TAPET) for diagnostic imaging. J Control Release 2001; 74(1-3): 313–315
29. Devraj B, Meenhard H. *Salmonella typhimurium* as a novel RNA interference vector for cancer gene therapy. Cancer Biol Ther 2008; 7(1): 151–152
30. Mei S, Theys J, Landuyt W, Anne J, Lambin P. Optimization of tumor-targeted gene delivery by engineered attenuated *Salmonella typhimurium*. Anticancer Res 2002; 22(6A): 3261–3266
31. Bhushan JT, Neil SF. Motility is critical for effective distribution and accumulation of bacteria in tumor tissue. Integr Biol 2012; 4(2): 165–167
32. Broadway KM, Suh S, Behkam B, Scharf BE. Optimizing the restored chemotactic behavior of anticancer agent *Salmonella enterica* serovar Typhimurium VNP20009. J Biotechnol 2017; 251: 76–83
33. Thamm DH, Kurzman ID, King I, Li Z, Sznol M, Dubielzig RR, Vail DM, MacEwen EG. Systemic administration of an attenuated, tumor-targeting *Salmonella typhimurium* to dogs with spontaneous neoplasia: phase I evaluation. Clin Cancer Res 2005; 11(13): 4827–4834